EFFECT OF RELATIVE VELOCITY BETWEEN ROUGH SURFACES: HYDRODYNAMIC LUBRICATION OF ROTARY LIP SEAL

I. LAHJOUJI[*], M. El GADARI, B. EL FAHIME and M. RADOUANI
Moulay Ismail University
High School of Engineering ENSAM Meknes
Research Laboratory in Mechanical, Mechatronic & Control – L2MC, MAROCCO
E-mails: imanelahjouji14im@gmail.com; m.elgadari@ensam-umi.ac.ma
b.elfahime@ensam-umi.ac.ma; m.radouani@ensam-umi.ac.ma

Since the sixties, most of numerical studies that model the rotary lip seal lubrication have been restricted by assuming that one of the two opposing surfaces is smooth: either the lip or the shaft. This hypothesis, although it is verified only for a shaft roughness ten times smaller than that of the seal, is the best solution to avoid the transient term "$\partial h/\partial t$" in the deterministic approach. Thus, the subject of the present study is twofold. The first part validates the current hydrodynamic model with the international literature by assuming the asperities on the lip and shaft as a two-dimensional cosine function. In the second part the Reynolds equation for rough surfaces with relative motion is solved. The numerical results show that the relative motion between rough surfaces impacts significantly the load support and the leakage rate, but affects slightly the friction torque.

Key words: hydrodynamic lubrication, roughness, relative velocity, Reynolds equation, finite differences.

1. Introduction

A lip seal device is the simplest and most widely used for sealing rotating shafts. Its role is to prevent leakage at low oil pressure without causing high dissipation or wear, but how it works is still not completely understood. This is due to the complex mechanisms of oil film formation between an elastomeric lip fitted with interference on a rotating shaft. When the two mating surfaces are in relative motion, the sealing and lubricating film must be present in the interference to avoid the wear effect. Indeed, previous studies have been done and shown that in steady state conditions the lip and the shaft surfaces are separated by a thin lubricating liquid film. Thereby, when the liquid is displaced to the top of each asperity, the film thickness varies and produces a rise in pressure on the upstream side, and cavitation on the downstream side [1]. In order to master the presence of two paradoxical phenomena, namely wear and leakage, several lubrication models have been studied, namely HD (Hydrodynamic), EHD (Elastohydrodynamic), TEHD (Thermo-Elastohydrodynamic), and VEHD (ViscoElastohydro-dynamic). In the transient condition, numerically, it is difficult to solve the Reynolds equation coupled to the thermal phenomenon and the mechanical behavior of the lip (viscoelastomeric or elastomeric).

It is important to note that modeling the lip lubrication with the elastohydrodynamic or viscoelastohydrodynamic behavior is complicated when the relative motion is considered. This is due to the inertia effect on the rotary lip spring elasticity, which is not neglected if the lip is moving. It is well known according to previous works [2, 3 and 4] that the influence coefficient matrix was computed by considering a stationary lip, and so far, no study has explained the lip inertia effect on the compliance matrix. This phenomenon will be discussed in the forthcoming papers.

---

[*] To whom correspondence should be addressed

Through the HD model, the Reynolds equation [2] was solved in the active and non-active zone by taking into consideration the lip and shaft roughness. A numerical analysis of the isothermal hydrodynamic lubrication was done by using the finite difference for spatial method and an implicit scheme for the temporal domain.

This paper intends to, on the one hand, identify the parameters related to shaft roughness that affect the lip seal life: load support and leakage rate by comparing these results with those of Shen [3] and on the other hand, investigates the effect of relative motion between the shaft and the lip on the rotary lip seal performances.

2. Hydrodynamic model

In this study we assume the following: The rotating shaft is considered rough, and the lip seal is aligned [4] (Fig.1).

In practice, the width contact ratio between the seal and the shaft is about 10^{-6}. This weak domain leads to numerical complications in meshing and solving the Reynolds equation (Fig.2). In order to avoid these limitations, we will consider a periodic roughness of the lip seal along the «*x*-axis » direction with a circumferential wavelength equal to «*L*». Therefore; a single cell with a length «*L*» and an axial contact width « *b* » is considered as new meshed domain. Thus, the global parameters were deduced by multiplying the local results and cell numbers.
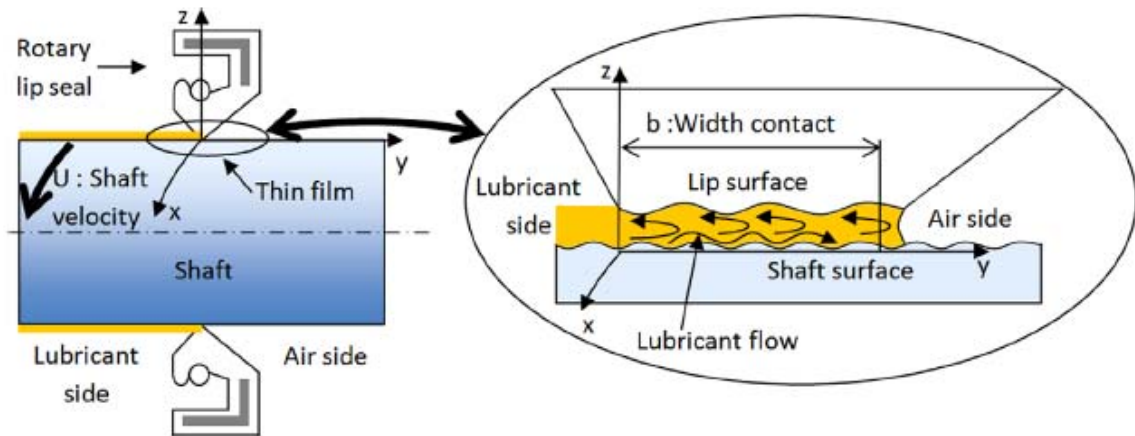

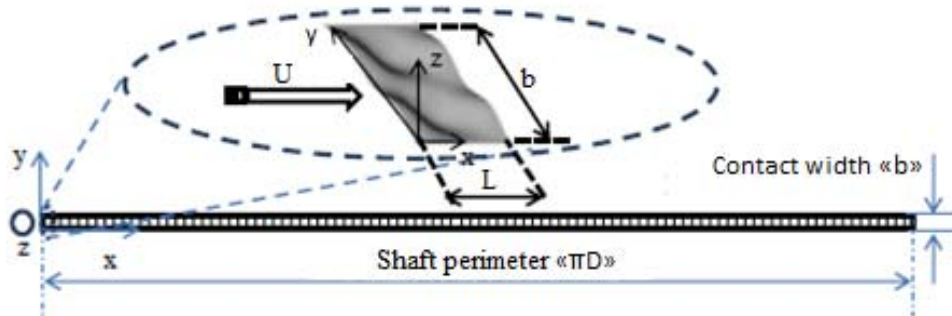Fig.1. Lip seal structure and location of the tightness area [5].

Fig.2. Domain of study.

2.1. Film thickness

The thickness of the film separating the lip seal and the shaft is calculated by deducting the lip roughness h_1 and the shaft roughness h_2 (Fig.3). Since the full film lubrication is taken into consideration, it is important to consider the average film thickness h_0 in order to neglect the contact between the asperities. The expression of the film thickness [2] is given by

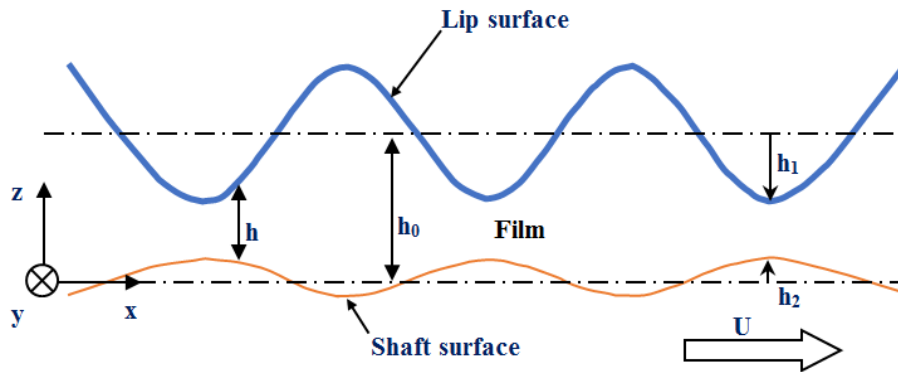$$h = h_1 - h_2 + h_0. \tag{2.1}$$

Fig.3. Film thickness.

2.2. Fluid mechanics

The generalized Reynolds equation characterizes the pressure field, where cavitation zones are assumed to be filled with a homogeneous lubricant-air mixture. The modified Reynolds equation

$$\frac{\partial}{\partial x}\left(h^3 F \frac{\partial D}{\partial x}\right) + \frac{\partial}{\partial y}\left(h^3 F \frac{\partial D}{\partial y}\right) = 6\mu U \frac{\partial h}{\partial x} + 12\mu \frac{\partial h}{\partial t} + 6\mu(1-F)\left(U \frac{\partial D}{\partial x} + 2 \frac{\partial D}{\partial t}\right). \tag{2.2}$$

In the active zone

$$D = p, \qquad D \geq 0,$$
$$F = 1, \tag{2.3}$$

in the cavitation zone (not active)

$$D = r - h, \qquad D < 0,$$
$$F = 0, \tag{2.4}$$

And
$$r = \frac{\rho_h}{\rho_0} \tag{2.5}$$

where "r" is the replenishment ratio, "ρ" is the lubricant density and "ρ_0" is the air density.

2.3. Lip and shaft roughness

In order to validate the current model, similar conditions as in Shen [3] were adopted. Thereby, the case of the rotating shaft and stationary rotary lip is assumed.

For this purpose, the surface roughness is considered as double sinusoidal function (Fig.5) and the average film thickness is equal to $1\mu m$. Thus, the lip roughness is modeled by

$$h_1(x,y) = A_1 \cos\left(\frac{2\pi}{L_{11}}(x - c_g)\right)\cos\left(\frac{2\pi}{L_{12}}y\right) \tag{2.6}$$

where cg is the shearing deformation of the lip, with

$$c_g = L_{11}\left(\frac{2y}{y_b} - \frac{y^2}{y_b^2}\right) \qquad \text{if} \qquad y < y_b,$$

$$\tag{2.7}$$

$$c_g = L_{11}\frac{\left(b^2 - 2y_bb + 2y_by - y^2\right)}{\left(b - y_b\right)^2} \quad \text{if} \quad y \geq y_b,$$

and yb represents the location of the maximum dry contact pressure (results of structural analysis with the commercial simulation software « Abaqus ») as shown in Fig.4.
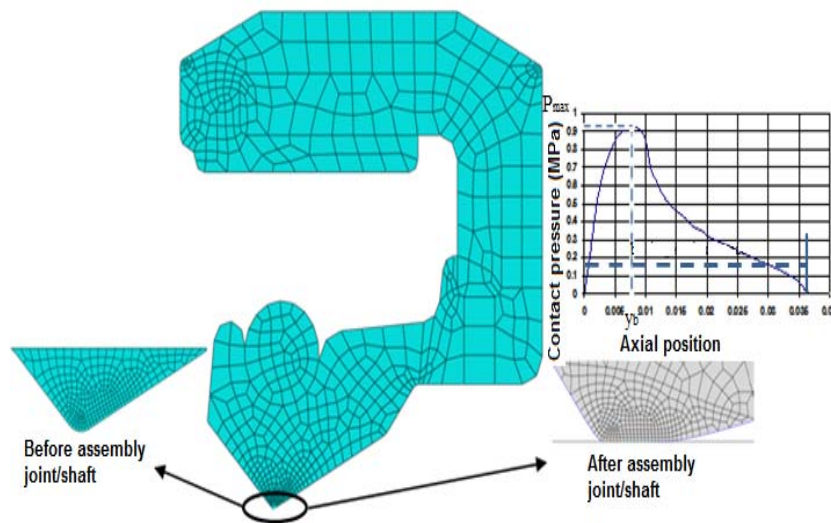

Fig.4. The maximum circumferential strain location [2].

We assume that the shaft roughness is given by

$$h_2(x,y,t) = A_2 \cos\left(\frac{2\pi}{L_{21}}(x - tU)\right)\cos\left(\frac{2\pi}{L_{22}}y\right). \tag{2.8}$$

The modified Reynolds equation is solved by the finite differences method [6] using the algorithm shown in Fig.6.
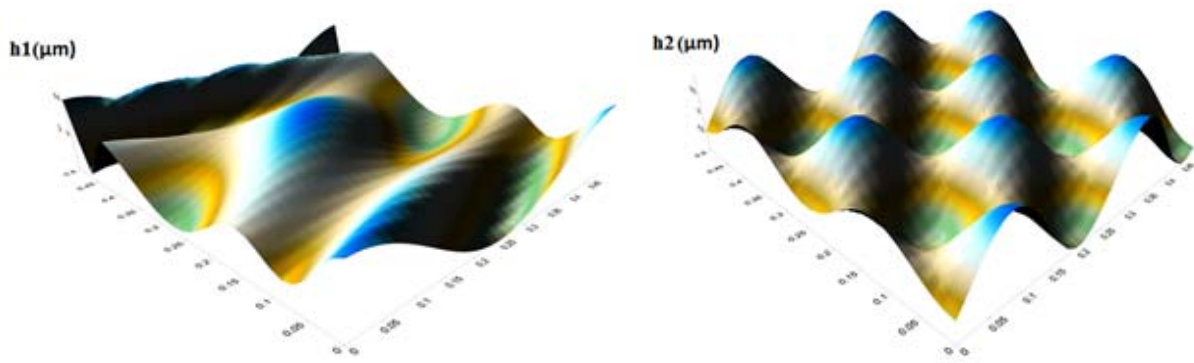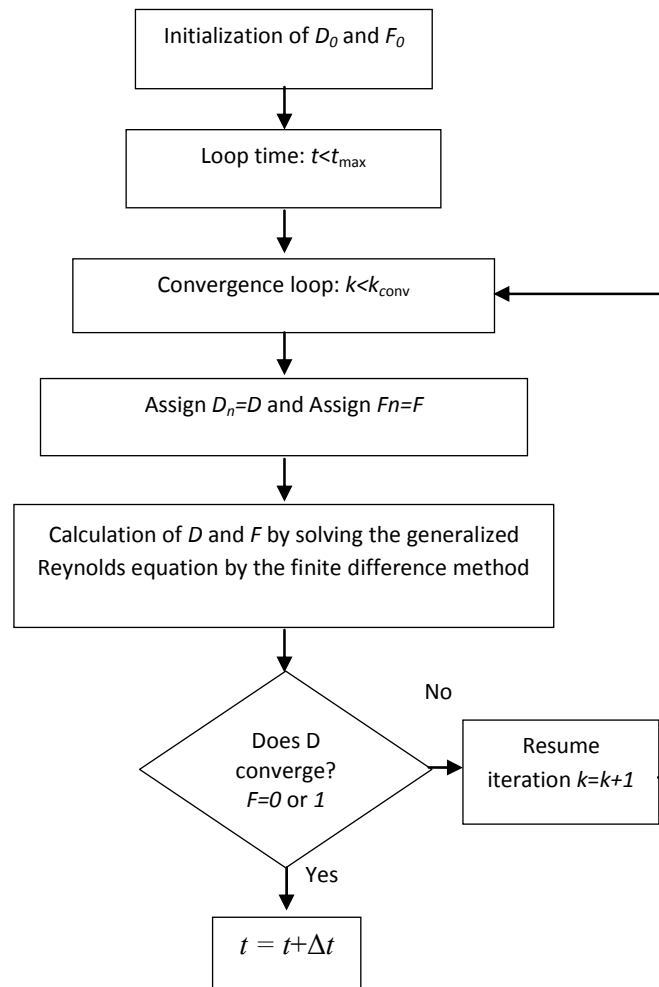
Fig.5. Lip and shaft roughness (h1& h2).

Fig.6. Flowchart for the solution of the Reynolds equation

When the Reynolds equation is solved, the lifting load "W", leakage rate "Q" (computed on the air and lubricant sides contact boundary) and friction torque "C" are calculated by [7].

$$W = \iint (p - p_a) \, dx \, dy, \tag{2.9}$$

$$Q = \int -\frac{h^3}{12}\frac{\partial p}{\partial y}dx ,\tag{2.10}$$

$$C = \iint \left(-\frac{1}{2}\frac{\partial P}{\partial x}h + \mu\frac{U}{h} \right)dx\,dy .\tag{2.11}$$

2.4. Finite differences model

The modified Reynolds equation (Eq.(2.2)) is discretized using the finite difference approach. The meshed domain is a rectangle, with length "L" and width "b" as shown in Fig.7.

Thereby, we discretize uniformly the cyclic cell to (Nx-1) elements according to the "x-axis" and (Ny-1) elements in the "y-axis". The time step is given by « Nt » partition throughout the time period.

Therefore, the Taylor-Young formulation is given by

$$\frac{\partial D}{\partial x} = \frac{D_n(i) - D_n(i-1)}{\Delta x} ,$$

$$\frac{\partial D}{\partial y} = \frac{D_n(i) - D_n(i-Nx)}{\Delta y} ,\tag{2.12}$$

$$\frac{\partial D}{\partial t} = \frac{D_n(i) - D_{n-1}(i)}{\Delta t}$$

where the nodal variable "X" is noted by $X_j(i)$, such as « i » is the index of the spatial node and « j » is the index of time.

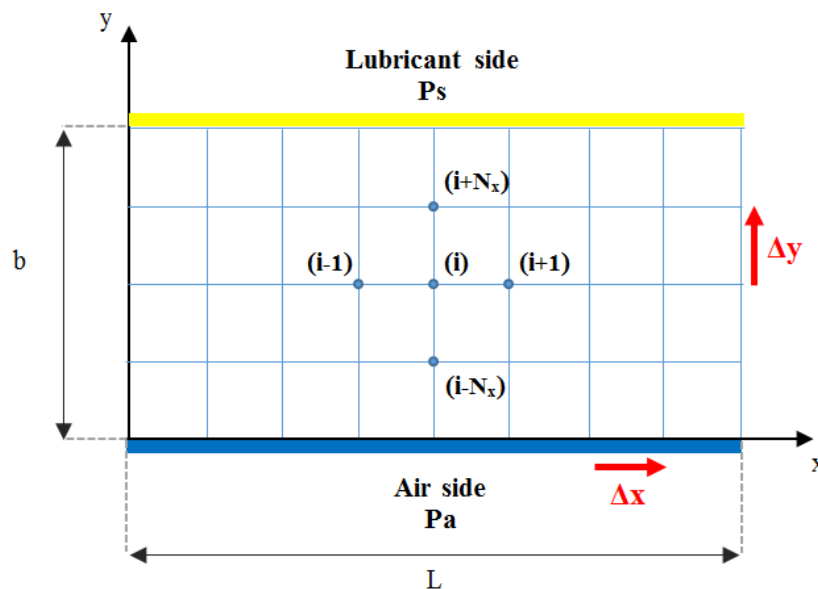The boundary conditions are given by: at $y=0$: $p=pa$; at $y=b$: $p=ps$.

Fig.7. Schematic representation finite differences mesh.

Thus the discretized Reynolds equation is given by

$$-AD_n(i) + BD_n(i+1) + CD_n(i-1) + ED_n(i+Nx) + KD_n(i-Nx) = G + HD_{n-1}(i) \qquad (2.13)$$

where

$$A = \frac{\left(2h_n^3(i) + h_n^3(i+1) + h_n^3(i-1)\right)F_n(i)}{2\Delta x^2} +$$
$$+\frac{\left(2h_n^3(i) + h_n^3(i+Nx) + h_n^3(i-Nx)\right)F_n(i)}{2\Delta y^2} + \frac{12\mu\left(1 - F_n(i)\right)}{\Delta t},$$

$$B = \frac{\left(h_n^3(i+1) + h_n^3(i)\right)F_n(i+1)}{2\Delta x^2} - 6\mu U \frac{\left(1 - F_n(i+1)\right)}{2\Delta x},$$

$$C = \frac{\left(h_n^3(i) + h_n^3(i-1)\right)F_n(i+1)}{2\Delta x^2} - 6\mu U \frac{\left(1 - F_n(i-1)\right)}{2\Delta x},$$

$$E = \frac{\left(h_n^3(i+Nx) + h_n^3(i)\right)F_n(i+Nx)}{2\Delta y^2},$$

$$K = \frac{\left(h_n^3(i) + h_n^3(i-Nx)\right)F_n(i+Nx)}{2\Delta y^2},$$

$$G = 6\mu U \frac{h_n(i+1) - h_n(i-1)}{2\Delta x} + 12\mu \frac{h_n(i) - h_{n-1}(i)}{\Delta t},$$

$$H = \frac{12\mu\left(1 - F_{n-1}(i)\right)}{\Delta t}.$$

The linear system is transformed into a matrix formulation:
$[M].D + R = \{0\}$, where $[M]$ is the stiffness matrix given by *A*, *B*, *C*, *E* and *K* and $[R]$ is the second right member. This system is solved by using an appropriate routine.

3. Validation code

In this section, a comparison between the current model results and the numerical simulations published in the international literature was made. For this purpose, the studied case of Shen [3] was reproduced. The parameters are: *b=0.5.10-4 m, L=0.5.10-4 m,* μ*= 2.5.10-2* Pa.s, *ps=1.02.105* Pa, *pa= ps=1.02.105* Pa, *A1=0.5.10-6 m, L11=b, L12=L, L22=b/2, L21=L/2, yb =3b/4*. A parametric study was

made in order to determine the nodes number according to the the *x*-axis and *y*-axis and the time step condition. Indeed, by choosing *Nx=Ny=30*, and time step number by period *Nt=30*, the numerical results are stabilized. The arithmetic roughness is given by

$$R_a\left(\text{lip}\right) = \frac{1}{bL} \iint |h_1(x,y)| \, dxdy \, ,$$

$$(3.1)$$

$$R_a\left(\text{shaft}\right) = \frac{1}{bL} \iint |h_2(x,y,t)| \, dxdy$$

where "| . |" is the absolute value.

Figure 8a represents the variation of time averaged load support divided by *W0* (the load support for a smooth shaft surface) versus the variation of the shaft roughness surface. It is shown that the load support rises significantly about *25%* when Ra (shaft) is *5%* of Ra (lip), and becomes stable by increasing the shaft roughness.
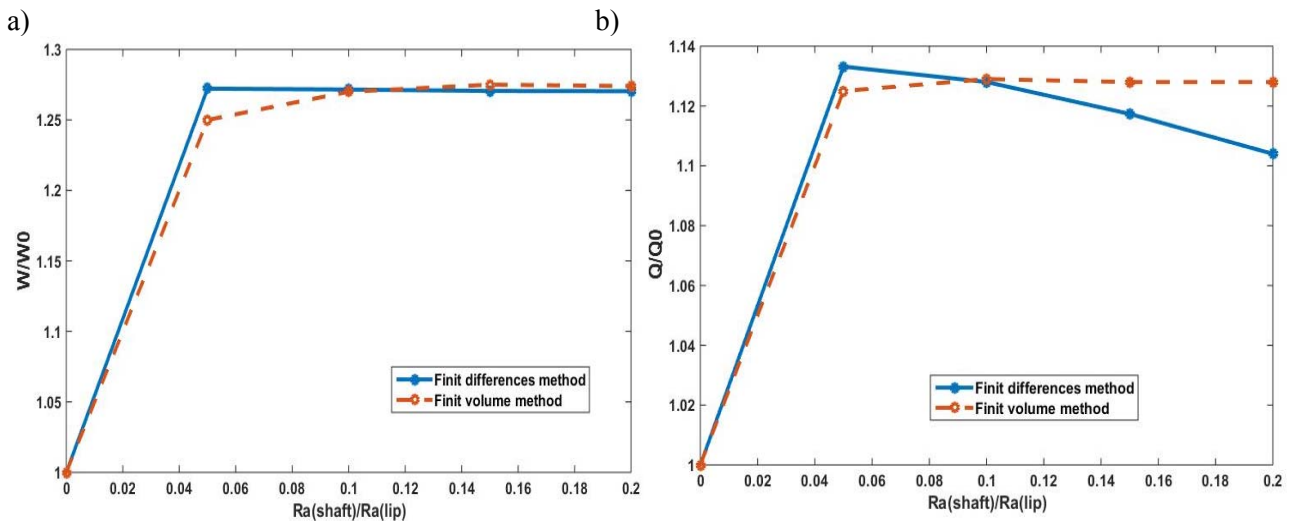

Fig.8. Effect of shaft surface on reverse pumping rate and load support.

Figure 8b shows the reverse pumping rate variation versus the shaft roughness ratio. It demonstrates that the reverse pumping rate is increased by *13.5%* compared to the smooth case when Ra (shaft) is *5%* of Ra (lip).

Thus, one deduces a good agreement between the current model results and the simulations performed by the finite volumes method [3]. The differences are about *0.36%* for the load support and *1.56%* for the reverse pumping rate.

After validating the present numerical approach, the relative motion effect of the shaft and lip surface is analyzed.

4. Effect of the shaft and lip motion

To investigate the effect of the shaft and the lip relative velocity on the hydrodynamic parameters, realistic roughness was used (Fig.9).

Indeed, the shaft and lip roughness were modeled with a randomized function with an average film thickness $h_0 = 3$ µm. The relative velocity of the shaft and lip surface is kept equal to *10 m/s* and three cases are distinguished (U_1 is lip velocity and U_2 the shaft velocity (Fig.10)) as follow
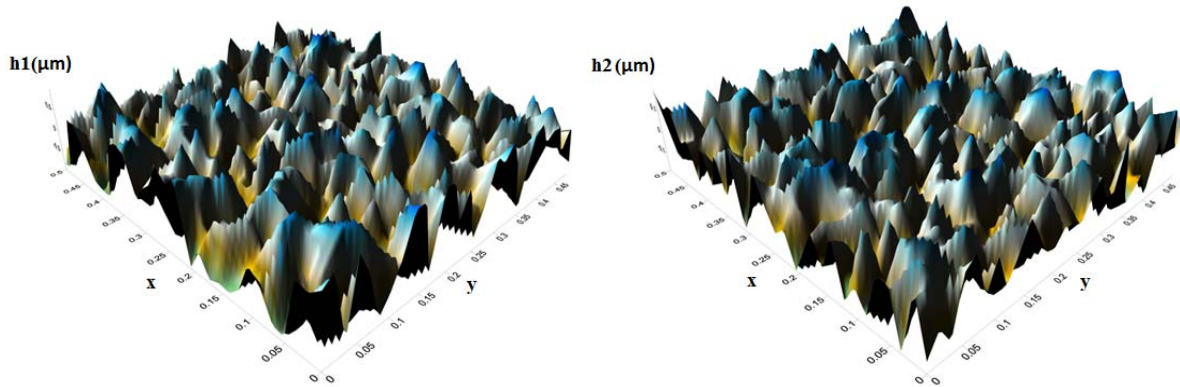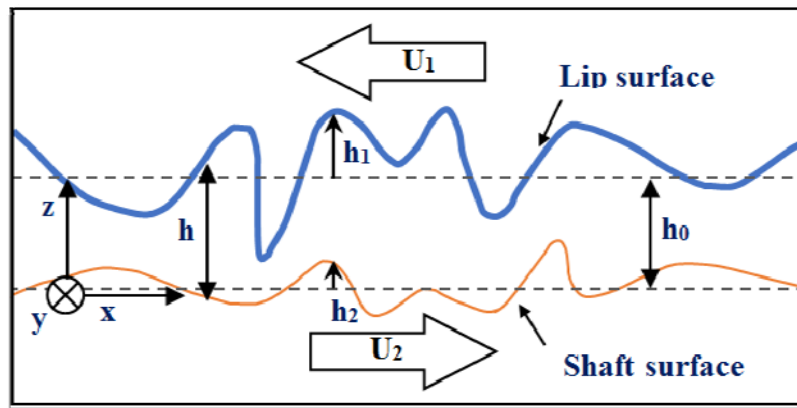

Fig.9. Realistic lip and shaft roughness.

Fig.10. Lip and shaft motion.

- Case #1: The shaft is stationary and the lip is moving with a negative speed *U1=-10 m/s, U2=0 m/s*.
- Case #2: The shaft is rotating with a positive velocity and the lip is immobile *U1=0 m/s, U2 = 10 m/s*.
- Case #3: The shaft and the lip are moving in opposite directions *U1=-5 m/s, U2=5 m/s*.
- Case #4: The shaft and the lip are moving in opposite directions with different velocities module *U1=10 m/s, U2=20 m/s*.

By considering the motion of the two surfaces, the Reynolds equation becomes [8]

$$\frac{\partial}{\partial x}\left(h^3 F \frac{\partial D}{\partial x} \right) + \frac{\partial}{\partial y}\left(h^3 F \frac{\partial D}{\partial y} \right) = 6\mu\left(U_2 + U_1\right)\frac{\partial h}{\partial x} + 12\mu\frac{\partial h}{\partial t} +$$
$$+6\mu\left(1 - F\right)\left(\left(U_2 + U_1\right)\frac{\partial D}{\partial x} + 2\frac{\partial D}{\partial t} \right). \tag{4.1}$$

The friction torque and active zone are given by

$$C = \iint \left(-\frac{1}{2}\frac{\partial p}{\partial x}h + \mu\frac{U_1 - U_2}{h} \right)dxdy \,, \tag{4.2}$$

$$ZA_n = \frac{\sum_{i=1}^{N}F_n(i)}{N} \,,$$

$$N = (N_x - 1)(N_y - 1) \,. \tag{4.3}$$

The lifting force "W/W_0", friction torque "C/C_0" and leakage ratio "Q/Q_0" were studied versus the shaft roughness "Ra(shaft)/Ra(lip)", the averaged values were computed throughout one period. It is necessary to note the index "$_0$" is the numerical result corresponding to the smooth shaft.

Figure 11 shows the effect of relative velocity between the lip and shaft surfaces on lubricant flow and lifting force. Indeed the reverse pumping and load support are underestimated when the lip or shaft surface is immobile and shaft motion is considered and overestimated when both surfaces are moving for both cases #3 and #4. This result confirms that moving both surfaces generates substantial hydrodynamic pressure and increases significantly the cavitation zone compared to the other cases (#1&#2).
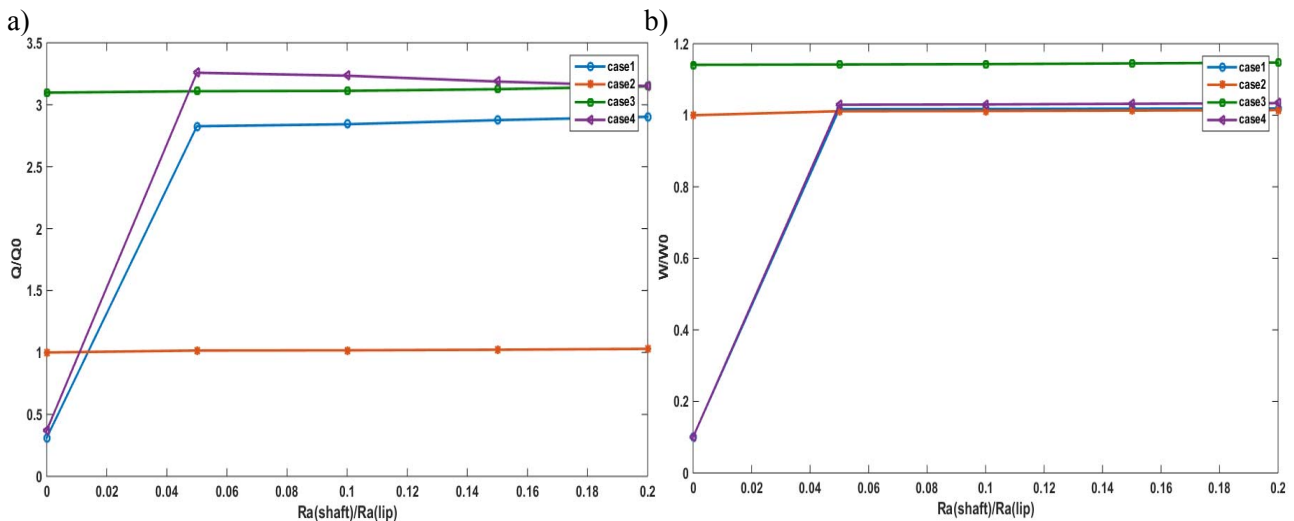

Fig.11. Reverse pumping and lifting force versus shaft arithmetic roughness: a) lubricant flow, b) lifting force.

Figure 12 shows that considering only the shaft or lip displacement produces a weak film pressure and an important active zone which can be compared to the cases when both surfaces are moving. The previous results are confirmed by Fig.13 which shows that the friction torque in the shaft surface is more significant when the shaft or the lip are considered stationary comparing to the cases when both are moving simultaneously.

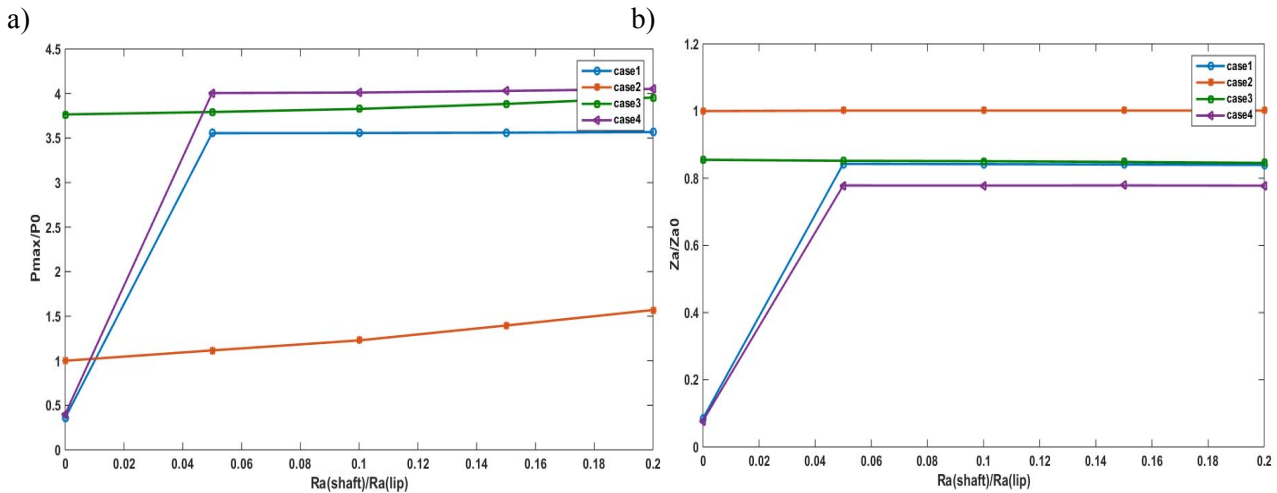a)   b)

Fig.12. Film pressure and active zone ratio versus shaft arithmetic roughness: a) maximum film pressure, b) active zone ratio.
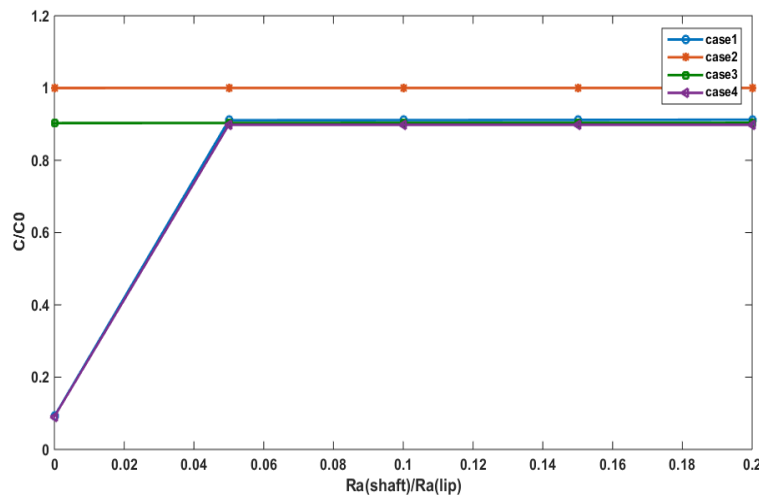

Fig.13. Friction torque versus shaft arithmetic roughness.

5. Conclusion

The aim of this work is to investigate the effect of rough surfaces in motion. On sealing mechanisms a good agreement has been shown between the current model and the results published previously in the international literature. By considering relative motion of the shaft and lip surfaces the rotary lip seal performances were studied. It was demonstrated that considering velocities of both surfaces, the hydrodynamic pressure and cavitation area increase significantly compared to the classical case: moving shaft and stationary lip. Consequently, the current hydrodynamic model confirms that moving both surfaces is needed for a successful rotary lip seal.

This result clearly indicates the importance of a judicious choice of the mating surfaces finish, and their relative motions in improving the performance and lifetime of the lip seal device. This study may suggest experimental testing in order to validate the hydrodynamic model as a simple and reliable tool to predict numerically the functioning of rotary lip seal with relative motion.

Nomenclature

A_1 – half amplitude of lip surface fluctuation [m]
A_2 – half amplitude of shaft surface fluctuation [m]
 b – width of solution space (sealing zone) in axial (y) direction [m]
 D – universal variable
 F – flag indicating cavitation zones
 L – length of solution space in circumferential (x) direction [m]
L_{11} – lip surface wavelength in x direction [m]
L_{12} – lip surface wavelength in y direction [m]
L_{21} – shaft surface wavelength in x direction [m]
L_{22} – shaft surface wavelength in y direction [m]
 P – pressure [Pa]
P_a – ambient pressure [Pa]
P_s – lubricant pressure [Pa]
 Q – reverse pumping rate [g/h]
Ra – average roughness height [m]
 U – speed [m/s]
 W – load support [N]
 x – axial coordinate [mm]
 y – circumferential coordinate [m]
y_b – axial location of maximum circumferential shear deformation of lip [m]
Z_a – the active zones rate
 μ – viscosity [Pa·s]

References

[1] Chen H., Wu Q., Xu C. and Zuo M. (2014): *Research on cavitation regions of upstream pumping mechanical seal based on dynamic mesh technique.* – Advances in Mechanical Engineering, vol.2014, Article ID 821058.

[2] El Gadari M. (2013): *Étude expérimentale et numérique du comportement des joints à lèvre.* – Sustained at Hassan II University, Morocco.

[3] Shen D. (2005): *Deterministic modeling of a rotary lip seal with microasperities on the shaft surface.* – Presented at the Academic University: Georgia Institute of Technology.

[4] Maoui A., Hajjam M. and Bonneau D. (2008): *Effect of 3D lip deformations on elastohydrodynamic lip seals behavior.* – Science Direct, Tribology International, vpol.41, pp.901-907.

[5] El Gadari M., Fatu A. and Hajjam M. (2015): *Shaft roughness effect on elasto-hydrodynamic lubrication of rotary lip seals: Experimentation and numerical simulation.* – Science Direct, Tribology International, vol.88, pp.218–227.

[6] Kouatchou J. (): *Finite Differences and Collocation Methods for the solution of two dimensional.* – NASA Goddard Space Flight Center, Code 931, Greenbelt, MD 20771.

[7] El Gadari M., Fatu A. and Hajjam M. (2016): *Effect of grooved shaft on the rotary lip seal performance in transient condition: Elasto-hydrodynamic simulations.* – Science Direct, Tribology International, vol.93, pp.411–418.

[8] Gherca A. (2013): *Modélisation de la lubrification des surfaces texturées : Application à la butée en régime hydrodynamique.* – Sustained at POITIERS University.